International Journal of Applied Mathematics

Volume 38 No. 5s, 2025

ISSN: 1311-1728 (printed version); ISSN: 1314-8060 (on-line version)

THE EFFECT OF OPENING POSITION AND STRENGTHENING TECHNIQUE ON WAFFLE SLAB BEHAVIOR

Abdullah Sikar Al-Issawi [1, a *], Najlaa Hameed Alshareef [2, b] and Abbas S. AL-Ameeri [3, c]

[1,2,3] Civil Engineering Department, University of Babylon, Babylon, Iraq

[a] abdullah.s.issawi@gmail.com, [b] eng.najlaa.hameed@uobabylon.edu.iq,

[c] abbas.alameeri.eng@uobabylon.edu.iq

Abstract

The behaviour of two-way waffle slabs with an eccentric aperture is studied in this paper. Basalt textile reinforced mortar (BTRM) was used to externally reinforce these slabs under simply supported boundary circumstances. The samples had measurements of 1050 x 1050 mm, with a particular topping thickness of 50 mm and joist size of 100 × 50 mm. The joists' bottoms had 1/8 mm of steel reinforcement, while the tops had mesh measuring 6 mm at 75 mm c/c.

Results showed that warping the catted ribs using the basalt fibre reinforced mortar approach greatly improved ductility and increased flexural strength when reinforcing ribs cut with square and circular openings.

1. Introduction

The structural limitations regarding waffle slabs integrity effecting directly on making openings in this slab system, this critical procedure needs further investigation specially when the main joists catted and stresses path altered [1].

FRP strengthening was the dominant procedure for past decades and this technique investigated with variety of polymers-epoxy matrices [2, 3]. A cement-based matrices that depends on inorganic mortars with fiber mesh introduced as environment and construction friendly replacement [4] [5].

(Ibrahim et al., 2009) concluded that the opening size may increase to 40% of the column strip width without substantially changing the moment capacity values [6].

Aguiar et al. (2021) studied waffle slabs with an opening and punching shear applied symmetrically. According to the findings, it is more beneficial to have an aperture that is close to the applied load in order to significantly reduce the slab's punching capacity than to increase the size or number of holes [7].

The behaviour of waffle slabs reinforced with CFRP sheets during punching shear testing was detailed in a study by Khamees and Abd Ali (2024). After undergoing the CFRP retrofitting technique, the punching shear capacity was considerably enhanced [3].

Received: August 03, 2025

International Journal of Applied Mathematics
Volume 38 No. 5s, 2025
ISSN: 1311-1728 (printed version); ISSN: 1314-8060 (on-line version)

This paper will give the results of an experimental and numerical analysis of the flexural behaviour of two-way waffle slabs, specifically looking at the effects of opening location and strengthening approach.

2. Experimental program

In this investigation, nine examples were used; each specimen had the following measurements: 100 × 50 mm for the joists, and 1050 × 1050 mm for the overall dimensions and accurate topping thickness. The steel reinforcement was organised in an orthotopic fashion, with ϕ6 mm mesh at the top and 1 ϕ8 mm at the bottom of the joists, as seen in figure (1).

The slabs were classified into control without opening (U) and and three with (150 mm) square opening at the center, RC slab without strengthening while RCNS and RCNB where strengthened with 8 mm rebar by implementing near surface mounted technique with steel and basalt rebar respectively.

two with (200 mm) square opening at the second rips intersection close to the edge, the first one without any strengthening (E2R200), and the other had a BTRM sheet on the joist around the open (E2R200B). specimens (E2R and E2RB) were the same as (E2R200 and E2R200B) except That had A (150 mm) opening.

Another slab contains a square (150 mm) opening positioned at the intersection of the first ribs (E1R). An opening without damaging ribs was investigated in (SER) in the first waffle bay from the solid centre.

A circular opening that had a (150 mm) diameter was investigated in three waffle slabs (E1C, E2C and E2CB) that had the precisely same properties as slabs (E1R, E2R, and E2RB) respectively.as shown in Fig. 1.

All slabs were subjected to a uniform distributed load under simply supported conditions from the four edges. Table (1) illustrates the slabs geometry.

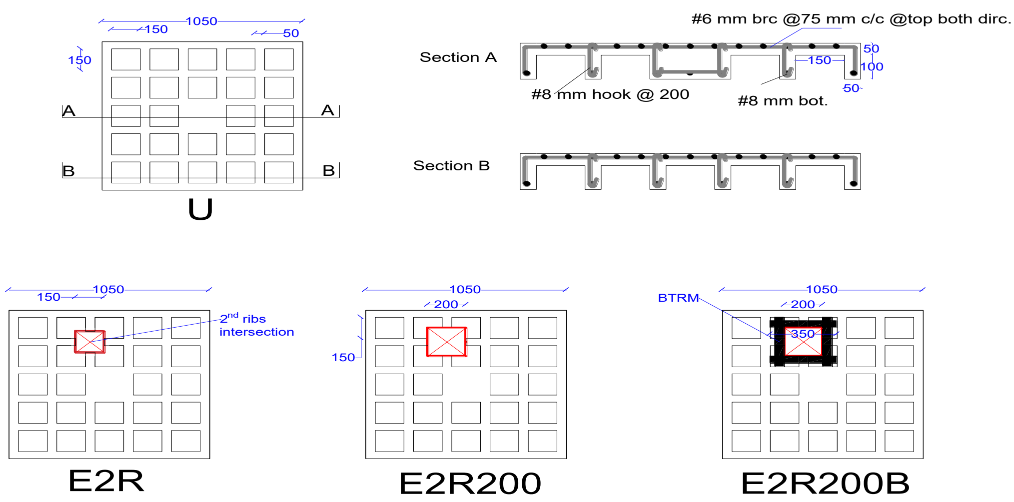

Received: August 03, 2025

Volume 38 No. 5s, 2025

ISSN: 1311-1728 (printed version); ISSN: 1314-8060 (on-line version)

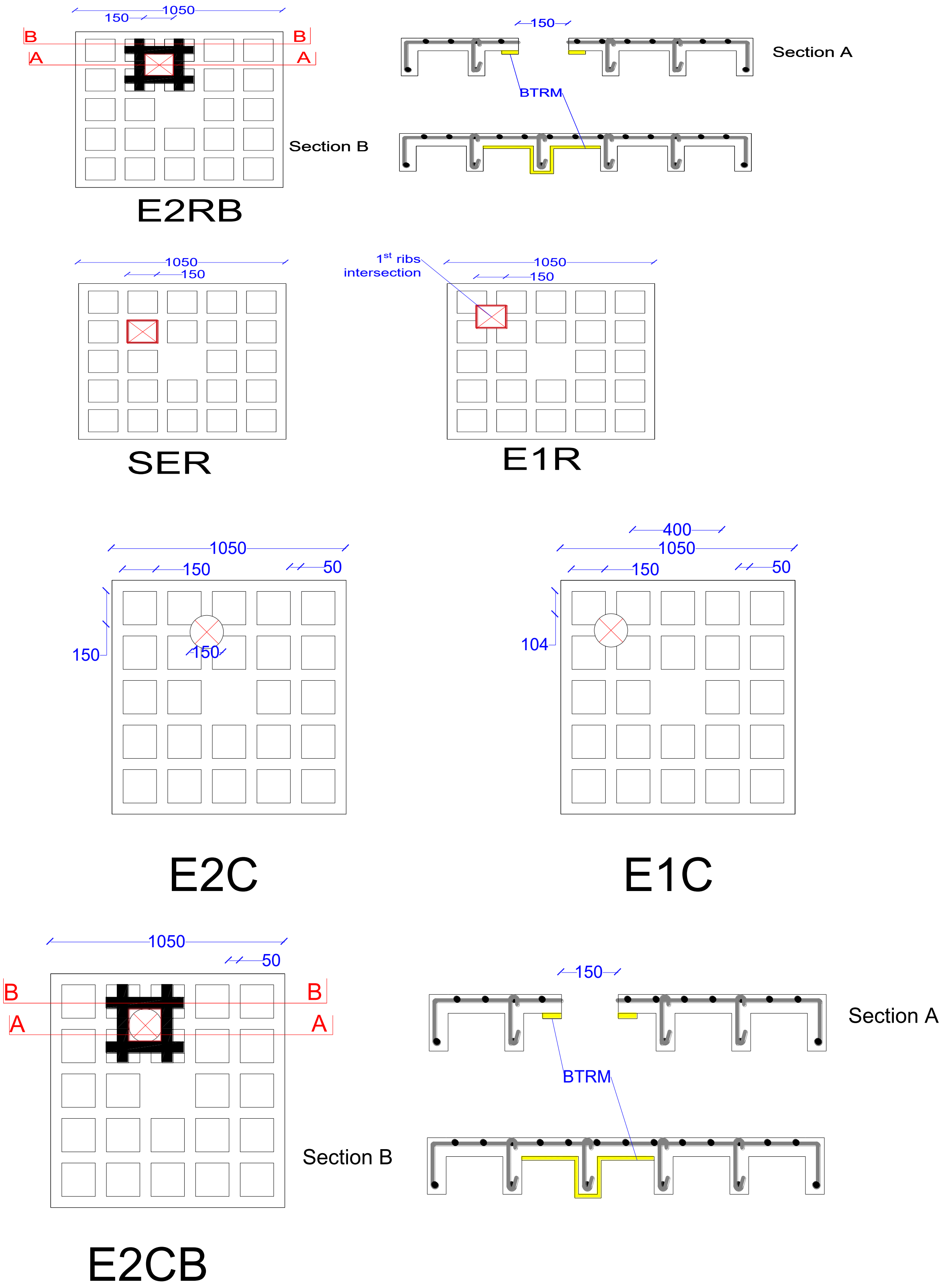

Fig.1 Slabs geometry

Received: August 03, 2025

Volume 38 No. 5s, 2025
ISSN: 1311-1728 (printed version); ISSN: 1314-8060 (on-line version)

Specimens	Opening size (mm)	Opening shape	Opening position	Strengthening
U	----	----	----	----
E2R200	200 x 200	Square	2nd ribs intersection	----
E2R200B	200 x 200	Square	2nd ribs intersection	BTRM
E1R	150 x 150	Square	1st ribs intersection	----
E2R	150 x 150	Square	2nd ribs intersection	----
E2RB	150 x 150	Square	2st ribs intersection	BTRM
SER	150 x 150	Square	Corner bay from the solid centre	----
E1C	150	Circle	1st ribs intersection	----
E2C	150	Circle	2nd ribs intersection	----
E2CB	150	Circle	2nd ribs intersection	BTRM

In the casting process of the waffle slab, normal concrete with (f'c =35 Mpa) and moisture cured until 28 days before strengthening. Steel rebar yielding and tensile strengths are shown in table (2)

Table 1. Specimens details

Table 2. Steel reinforcement properties

Bar diameter	Fy (Mpa)	Fu (Mpa)
6	350	470
8	430	546

The formwork was prepared, and pressurized cork cubes made the waffle bays, as shown in Fig. 2.

Received: August 03, 2025

International Journal of Applied Mathematics

Volume 38 No. 5s, 2025

ISSN: 1311-1728 (printed version); ISSN: 1314-8060 (on-line version)

Fig.2 Waffle formwork

Cement-based polymer-modified mortar (Cermirep R4 T) was used as an adhesive in basalt textile reinforced mortar (BTRM) with high compressive and adhesion stresses, This fibre-reinforced mortar combines specialised cements, high-purity silica sand, and fibre-reinforced additives as listed in Table 3. At the same time, basalt mesh consists of a (5 mm) square textile with high tensile stress fibre, which has properties in Table 4.

Before applying mortar, the concrete surface was rubbed until a rough surface was achieved, and then (50 mm) strips were submerged into the mortar see Fig. 3. Then, moisture curing (28 days) took place for the mortar.

Table 3. Mortar properties

Dry density	Compressive strength (1 day)	Compressive strength (28 days)	Flexural Strength (28 days)	Tensile Adhesion Strength	Modules of elasticity
1.75 kg/l	18 MPa	65 MPa	≥10 MPa	≥ 2.0 MPa	34.2 GPa

Table 4. Basalt mesh properties

Mesh size	Tensile Strength	Ultimate strain	Tensile modulus of elasticity
5 x 5 mm	830 MPa	2.8 %	29 GPa

Fig.3 BTRM installation

4. Results and discussion

Here are the experimental findings of the specimens that were tested: Table (5). It was detailed the cracking load, maximum loading capacity, failure mechanism, and maximum deflection that had been observed. All slabs exhibited flexural failure with rib breaking as their main behaviour.

Received: August 03, 2025

International Journal of Applied Mathematics
Volume 38 No. 5s, 2025
ISSN: 1311-1728 (printed version); ISSN: 1314-8060 (on-line version)

Table 5. Experimental results

specimens	Cracking load Pcr (kN)	Failure load Pu (kN)	Decreasing in loading capacity %	Crack width at 0.65 Pu (mm)	Max crack width (mm)	Max deflection (mm)	failure mode
U	85	405	-----	0.38	4.03	21.07	flexural failure with ribs cracking
E2R200	56	293	27.65	0.36	2.7	16.47	
E2R200B	67	318	21.48	0.28	3.1	21.52	
E1R	74	319	21.23	0.36	3.4	18.89	
E2R	70	307	24.20	0.31	3	18.57	
E2RB	77	345	14.81	0.35	4.7	24.95	
SER	80	384	5.19	0.38	3.5	24.88	
E1C	77	325	19.75	0.27	3.1	18.68	
E2C	73	313	22.72	0.37	2.7	18.37	
E2CB	78	357	11.85	0.33	2.4	24.3	

Cracks pattern

In accordance with the general deformation structural effect, there were three distinct phases to the cracking performance of the two-way waffle slabs. Elastic deformation predominates on the slabs at the outset of the applied loading, which is both concentrated and equally distributed. This is true until the first fracture emerges on the ribs near the solid area in the middle zone.

The cracks begin to expand and spread during the elastoplastic stage, eventually covering most of the ribs. This process continues until the plastic stage, which is characterised by faster crack propagation and bigger cracks than earlier phases.

According to the findings, when it came to the identical concrete materials, the opening location was the most effective parameter for cracking patterns. The fissures tend to propagate inwards and are only seldom seen close to the margins, across the first ribs' intersection aperture (E1) slabs (E1R and E1C)..

Since cutting the ribs influenced tensile stress transfer, the first cracks hold their positions in the central zone. Regarding the second rib (E2) intersection opening (E2R and E2C), the effect was more considerable than the (E1) opening, resulting in a more unsymmetric distribution of cracks around the opening zone.

Received: August 03, 2025

Volume 38 No. 5s, 2025

ISSN: 1311-1728 (printed version); ISSN: 1314-8060 (on-line version)

The slab (SER), which had an opening on the first waffle bay near the solid centre, was surrounded by ribs and performed similarly to the control slab (U). It had a higher loading capacity than all other opening positions, with cracks spreading and a larger width.

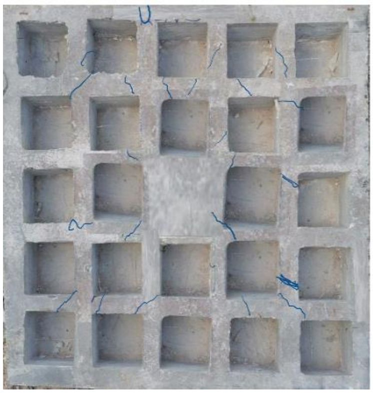

U

E2R200

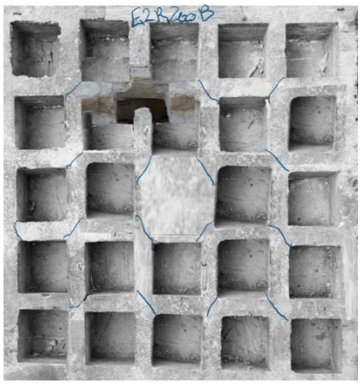

E2R200B

E1R

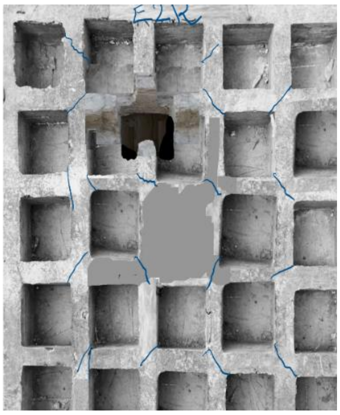

E2R

E2RB

SER

E1C

E2C

Received: August 03, 2025

International Journal of Applied Mathematics

Volume 38 No. 5s, 2025

ISSN: 1311-1728 (printed version); ISSN

E2CB

Fig. 4 Cracked slabs

Cracks width

You can see how cracks develop from when they first appear until they fail in Fig. 5, which shows the curves of maximum crack width versus load for all slabs. In contrast to the other slabs with holes, control slab U showed a greater envelope, and SER followed a similar pattern. As a result of the enhanced energy absorption brought about by BTRM strengthening, however, E2RB had the widest fracture width.

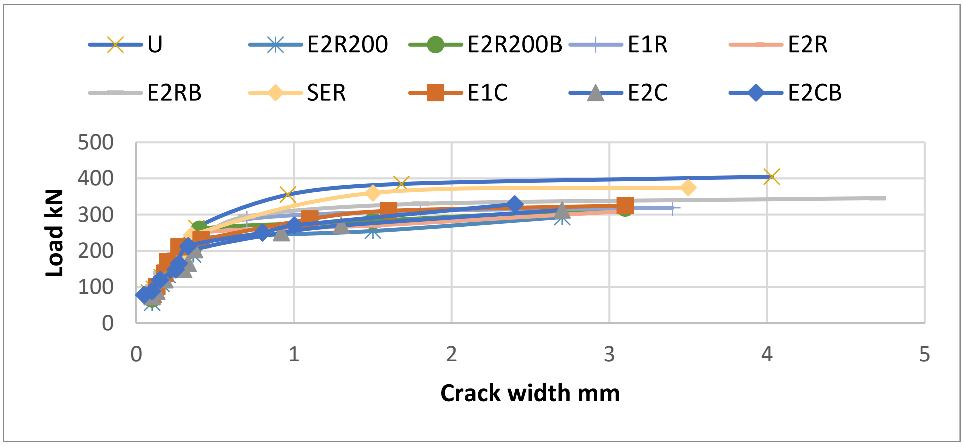

Fig. 5 max cracks width

Load deflection behavior

Figure 6's load-deflection curves showed elastic behaviour at the outset, however the first cracking occurred at (19.11-23.7)% of the failure load, which affected the subsequent three-phased curves. Rapid displacement data recordings with little load growth occurred when the steel reinforcement achieved yielding stress and the plastic phase—the last phase in slabs—became prominent.

Regarding ultimate loads and their related deflection, test findings do not show a significant difference between square and circular holes. Slabs (E1C) with round openings had a 1.9% and 1.9% improvement in loading capacity compared to those with square openings (E2C), but more extensive research is needed to fully understand how different opening shapes affect waffle slabs.

Received: August 03, 2025

Volume 38 No. 5s, 2025

ISSN: 1311-1728 (printed version); ISSN: 1314-8060 (on-line version)

The opening position seems to be a substantially effective parameter for loading capacity for the tested specimens. Changing the position of the openings (with the same size) from the second to first ribs intersection was combined with significant loading capacity raising and a considerable deflection increase, which achieved more ductility. Waffle slabs (E1C and E1R) had higher failure loads than (E2C and E2R) by (3.9 % and 3.8 %).

Cutting the opening surrounded by ribs in the slab, SER was sufficient to prevent slab capacity deterioration, with only a (5.18 %) lower failure load from solid slab U. Other slabs recorded a lower percentage (11.85 % to 27.6 %).

Reducing the opening size from 200 mm to 150 mm improved the load capacity of waffle slabs and enhanced the final deflection. For non-strengthened slabs, E2R had a higher failure load of 4.78 % than E2R200. Implementing BTRM strengthens the difference between E2RB and E2R200B, which is 8.49 %.

5. Finite Elements Analysis

An advanced finite elements (FE) computer program, Abaqus/CAE 2019, was used in this research. A 3D finite element analysis of the experimentally investigated waffle slab specimens was carried out to investigate model accuracy in predicting their behavior. In addition, several parameters were studied theoretically after verifying the validity of FEA.

Parts Assembly

The modelling of slabs involves drawing various parts depending on the geometry and properties of the experimental component of waffle specimens. All the parts were assembled in their proper positions.

Abaqus/CAE 2019 default element definitions were adopted to solve multiple non-linearity problems and adequately match the recorded results. (C3D8) brick linear eight-node elements were used to model concrete and plates. Meanwhile, (T3D2), a linear two-node truss element, was adopted to model the NSM technique's reinforcement and rebar. To model BTRM, a 4-node doubly curved thin or thick shell (S4R) element was implemented.

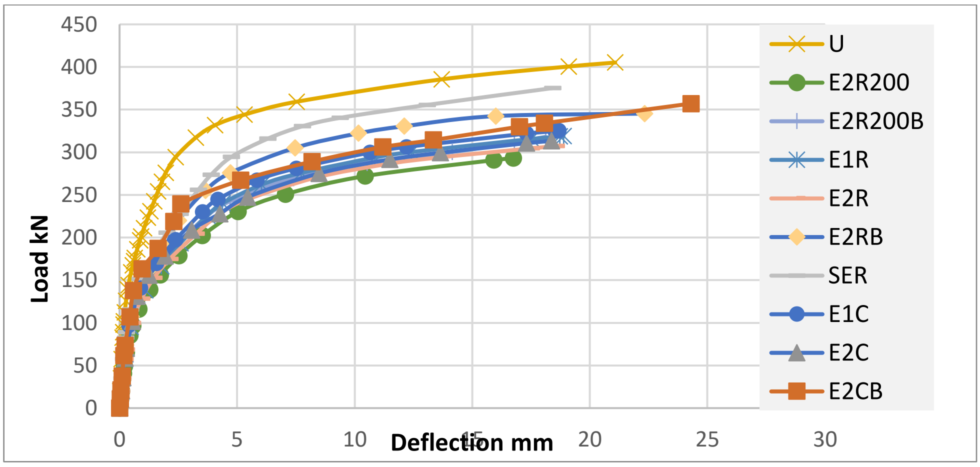

Fig. 6 Load-deflection curves

Received: August 03, 2025

Volume 38 No. 5s, 2025

ISSN: 1311-1728 (printed version); ISSN: 1314-8060 (on-line version)

Material Properties

The structural element's components' stress-strain behavior and contact characteristics influence its performance and behavior. To simulate material behavior, the following methods were used: Homogeneous sections were assumed for the solid parts, and laboratory tests on steel and concrete were conducted to assess their properties.

Concrete: Abaqus/CAE provided three different concrete models. The concrete damage plasticity CDP was adopted, representing concrete compressive crushing and tensile cracking behaviour.

Depending on the [8] model, the compressive stress-strain input contains damage parameters (dc) that refer to material stiffness loss. The stress-strain relationship of concrete in tension was modelled by using a relation suggested by [9] and modified [10] Fig.7 shows compressive and tensile curves versus inelastic strain. The plasticity parameters were calibrated according to data presented by [11].

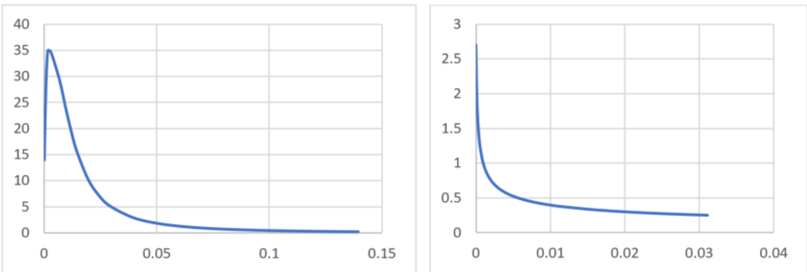

Fig.7 Compressive and tensile curves versus inelastic strain.

Basalt Textile Mortar

Depending on the three-phase stress-strain curve model originally reported by [12], illustrated in Fig.8 and reproved experimentally by [13], BTRM stresses numerical inputs adopted this model with the following equations.

First stage:

$$\sigma = E_{c1}\varepsilon = \left(E_f V_f + E_m V_m\right)\varepsilon \left(0 \leq \varepsilon \leq \varepsilon_{mu} = \frac{\sigma_{mu}}{E_m}\right) \ldots \ldots (1)$$

Where E_f and E_m represent the elastic moduli of the textile and mortar, respectively; V_f and V_m denote the volume fractions of the textile and mortar; σ_{mu} signifies the tensile failure stress of the mortar; ε_{mu} indicates the ultimate tensile strain of the mortar.

Second stage:

$$\sigma = \sigma_{mc} = \frac{E_{c1}\sigma_{mu}}{E_m}\left(\varepsilon_{mu} < \varepsilon < \varepsilon_{mc} = \frac{\frac{\sigma_{mc}}{V_f} - k_t \frac{\sigma_{mu}}{V_f}\left(1 + \alpha_e \cdot V_f\right)}{E_f} + \varepsilon_{mu}\right) \ldots (2)$$

Received: August 03, 2025

International Journal of Applied Mathematics

Volume 38 No. 5s, 2025

ISSN: 1311-1728 (printed version); ISSN: 1314-8060 (on-line version)

Where ε_{mc} denotes the multiple cracking strain, which is the composite strain after stage II; σ_{mc} represents the multiple cracking stress, indicating the stress at the end of stage II; k_t is an empirical factor valued at 0.2; E_f is the elastic modulus of the textile; and α_e is the ratio of the elastic modulus of the textile to that of the matrix.

Third stage:

$$\sigma = \frac{V_f E_f(\varepsilon - \varepsilon_{mc})}{\left[1 + \left(\frac{E_f(\varepsilon - \varepsilon_{mc})}{E_f \cdot \varepsilon_u}\right)^n\right]^{\frac{1}{n}}} + \sigma_{mc} \ldots\ldots(3)$$

Where ε_u is the failure strain value of the basalt TRM specimens, n equals 4, determined empirically. The modelling of the BTRM matrix depends on a layup composite that considers the material's orthotropic properties.

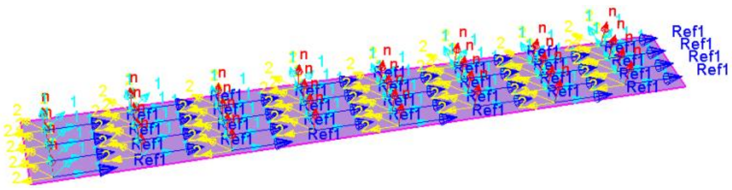

Fig.8 BTRM layup composite

FE Results

By comparing the FE results with the experimental data, an acceptable tolerance was recorded for waffle slab specimens, as listed in Table 6. The behavior of numerical load-deflection curves revealed a stiffer envelope than experimental tests. That is due to assumed homogeneous material characteristics and perfect theoretical bond between waffle slab components.

Microcracks formed by shrinkage and slab handling, in addition to the inability to measure the full stress-strain of concrete, also maximize the difference in stiffness. Previous reasons led to considering reasonable agreement between numerical and experimental curves, as shown in Fig.9.

Table 6. FE Results

SLAB	PU, EXP. (KN)	PU, FE (KN)	$\frac{\text{Pu, FE}}{\text{Pu, Exp.}}$	Δ EXP. (MM)	Δ FE (MM)	$\frac{\Delta\text{FE}}{\Delta\text{Exp.}}$
U	405	403.00	1.00	21.08	16.21	0.77
E2R200	293	290.67	0.99	16.74	10.98	0.66
E2R200 B	318	317.40	1.00	18.12	16.56	0.91
E2R	307	303	0.99	18.57	12.80	0.69

Received: August 03, 2025

International Journal of Applied Mathematics

Volume 38 No. 5s, 2025

ISSN: 1311-1728 (printed version); ISSN: 1314-8060 (on-line version)

E1R	**319**	**330.30**	**1.04**	**18.88**	**16.40**	**0.87**
E2RB	**345**	**340.20**	**0.99**	**22.32**	**16.30**	**0.73**
SER	**375**	**384.17**	**1.02**	**18.42**	**19.14**	**1.04**
E1C	**325**	**343.90**	**1.06**	**18.68**	**17.27**	**0.92**
E2C	**313**	**319.25**	**1.02**	**18.37**	**12.80**	**0.70**
E2CB	**357**	**370.20**	**1.04**	**24.3**	**22.40**	**0.92**

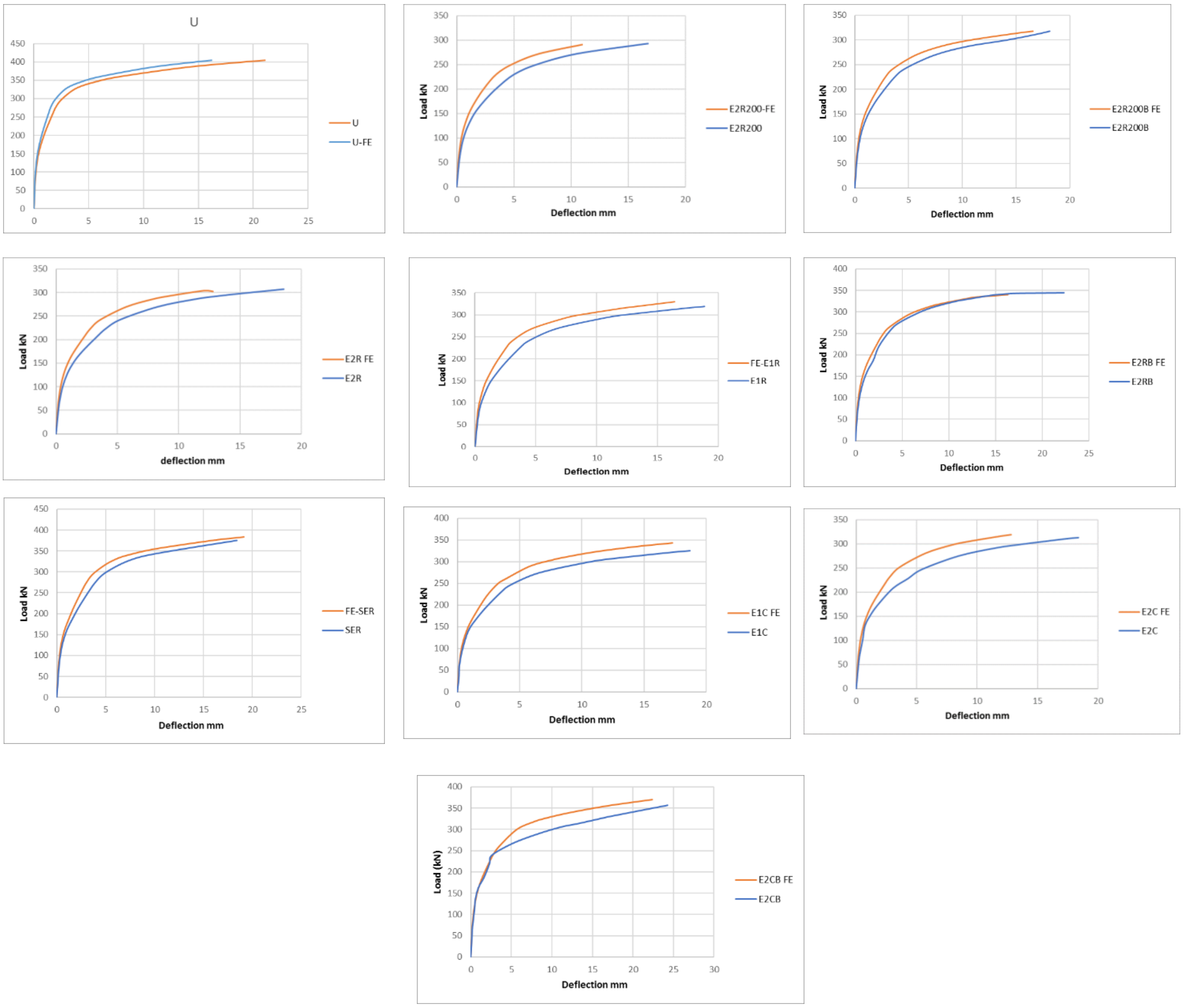

Fig.9 Experimental vs Numerical load-deflection curves

Parametric Study

After determining FEA's ability to predict two-way waffle slab structural behavior, several parameters affecting this system will be investigated numerically. Due to the practical

Received: August 03, 2025

Volume 38 No. 5s, 2025
ISSN: 1311-1728 (printed version); ISSN: 1314-8060 (on-line version)

importance of investigating these parameters that increase knowledge field about studying critical cases and optimizing the geometry of waffle slab

Eliminate Slab Corner

This numerical study eliminated a 200 mm square opening from the waffle slab corner under two different loadings. The UDL slab was donated as (UCR200 FE), while the slab under central loading will be (PCR200 FE). This edge-eliminating process leads to the investigation of unsymmetrically supported waffle slabs, as shown in Fig. 10 FEA results for both loading cases showed that the corner opening performed superiorly to the 200 mm opening in the E2 position, with higher loading capacity and energy absorption, as illustrated in Fig. 11.

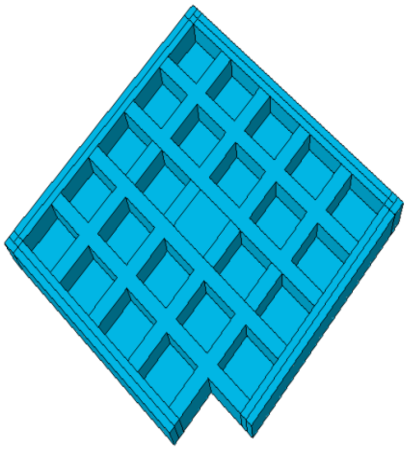

Fig. 10 Cutting corner opening in waffle slab

This is due to a continuous rib grid that does not cat by opening. Regarding the solid control slabs U FE and PFE, numerical results showed a lower loading of (6.2 and 9 %) and deflection of (19 and 26.7%) respectively. This insignificant tolerance makes edge opening the most practical position when several choices are available for the designer, although experimental investigation on real-scale slabs must be widely studied to cover edge elimination drawbacks.

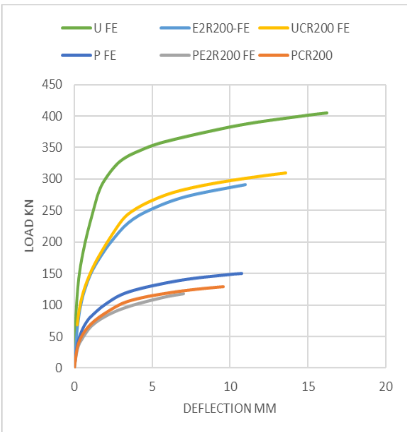

Fig. 11 Load-deflection for corner opening study

Received: August 03, 2025

International Journal of Applied Mathematics

Volume 38 No. 5s, 2025

ISSN: 1311-1728 (printed version); ISSN: 1314-8060 (on-line version)

5.4.4 Horizontal Ribs Cutting

No literature was available to investigate horizontal rib opening for monolithic concrete two-way waffle slabs, although this case is highly demanded for service ducts and pipes. Waffle slab geometry requires higher floors than other slab types. Hence, rib opening is the only solution in critical cases.

A parametric study, which would have given a better understanding of this severe geometry altering of the waffle slab, will be carried out in two suggested cutting paths.

Fig. 12 shows that specimen E1H had a cutting path that eliminated a full rib action in one direction and catted the perpendicular ribs with a 150 mm-wide boundary. This led to redistribute moments and losing waffle slab behaviour, with concrete splitting failure along the catted path at (229 kN) and that lower than (E1R FE) by 30 %.

Adequate suggestion by cutting only transverse ribs without harming the perpendicular direction is also modelled numerically. Slab (E2H) geometry had lowering cutting action but moved the path to more critical moment levels closer to midspan.

Failure load was recorded at (271.7 kN), with a higher load capacity and deflection than model E1H by (18.6 and 9.8 %). The favourable structural response clearly states that rib elimination should be avoided, and the cutting process should be optimised towards higher moment zones if conflicted with it.

The BTRM strengthening was introduced into model E2HB on the cutting path surrounding the ribs soffit. Since the critical zone and the failure action were at the opening path's topping, no stiffness increase yielded. The slab failed with higher deflection than E2H but with insignificant loading carrying capacity. Fig.13 demonstrates the load-deflection curves of this study.

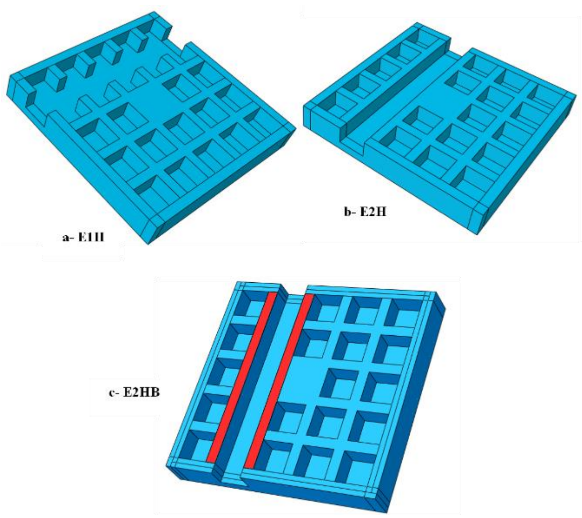

Fig.12 Numerical specimens of horizontal ribs opening

Received: August 03, 2025

ISSN: 1311-1728 (printed version); ISSN: 1314-8060 (on-line version)

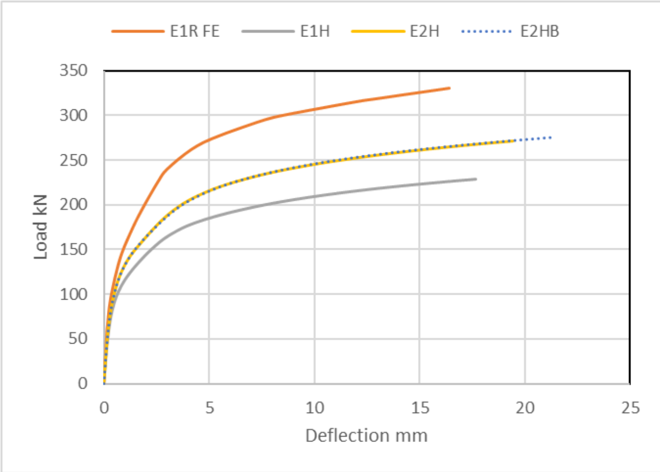

Fig. 13 Load-deflection for horizontal ribs opening

Conclusions

- In comparison to the catted opening of the second rib intersection (E2 type), the opening located in the first rib intersection (E1 type) exhibited stiffer behavior .

- The position of the opening appears to be a highly effective parameter for the loading capacity of the tested specimens.

- The BTRM method of warping the catted ribs significantly enhanced ductility, stiffness, energy absorption and flexural strength. The BTRM technique had a marked impact on waffle slab strengthening and improved structural behavior, with no evidence of matrix debonding observed.

- At the same geometric conditions, a large opening (200 mm) results in a noticeable drop in stiffness and loading capacity compared to a smaller opening (150 mm).

- Despite being the closest opening to the slab centre, the hole surrounded by ribs, as in the (SER) slab, exhibits a higher loading capacity and stiffness.

References

1. Abdul-Wahab, H.M. and M.H. Khalil, *Rigidity and strength of orthotropic reinforced concrete waffle slabs.* Journal of Structural Engineering, 2000. **126**(2): p. 219-227.

2. Jeenu Mary, V. and s. Soni, *Analytical study on strengthening of waffle slab with opening using CFRP sheets and stiffening ribs.* International Research Journal of Engineering and Technology (IRJET), 2016. **3**(9).

3. Khamees, R.S. and M.S. Abd Ali, *Experimental Study of Punching Shear on Reinforced Concrete Waffle Slabs Strengthened by CFRP Sheets.* Tikrit Journal of Engineering Sciences, 2024. **31**(3): p. 105-116.

4. Papanicolaou, C., et al., *Strengthening of two-way reinforced concrete slabs with textile reinforced mortars (TRM).* 2009.

Received: August 03, 2025

Volume 38 No. 5s, 2025

ISSN: 1311-1728 (printed version); ISSN: 1314-8060 (on-line version)

5. Tetta, Z.C., L.N. Koutas, and D.A. Bournas, *Textile-reinforced mortar (TRM) versus fiber-reinforced polymers (FRP) in shear strengthening of concrete beams.* Composites Part B: Engineering, 2015. **77**: p. 338-348.

6. Ibrahim, A., H. Salim, and H.S. Eldin. *Analysis of Waffle Slabs with and without Openings*. in *Structures Congress 2009: Don't Mess with Structural Engineers: Expanding Our Role*. 2009.

7. Aguiar, A., et al., *Punching shear strength of waffle flat slabs with opening adjacent to elongated columns.* Engineering Structures, 2021. **243**: p. 112641.

8. Wahalathantri, B., et al. *A material model for flexural crack simulation in reinforced concrete elements using ABAQUS*. in *Proceedings of the first international conference on engineering, designing and developing the built environment for sustainable wellbeing*. 2011. Queensland University of Technology.

9. Wang, T. and T.T. Hsu, *Nonlinear finite element analysis of concrete structures using new constitutive models.* Computers & structures, 2001. **79**(32): p. 2781-2791.

10. Kmiecik, P. and M. Kamiński, *Modelling of reinforced concrete structures and composite structures with concrete strength degradation taken into consideration.* Archives of civil and mechanical engineering, 2011. **11**(3): p. 623-636.

11. Michał, S. and W. Andrzej, *Calibration of the CDP model parameters in Abaqus.* World Congr Adv Struct Eng Mech (ASEM 15), Incheon Korea, 2015.

12. Larrinaga, P., et al., *Non-linear analytical model of composites based on basalt textile reinforced mortar under uniaxial tension.* Composites Part B: Engineering, 2013. **55**: p. 518-527.

13. Li, B., et al., *Tensile behavior of basalt textile grid reinforced Engineering Cementitious Composite.* Composites Part B: Engineering, 2019. **156**: p. 185-200.

Received: August 03, 2025